

Water Vapor Absorption of Electromagnetic Radiation in the Centimeter Wave-Length Range†

GORDON E. BECKER* AND STANLEY H. AUTLER

Columbia Radiation Laboratory, Columbia University, New York, New York

(Received May 20, 1946)

The water vapor absorption line resulting from the rotational transition $5_{-1}-6_{-5}$ has been investigated experimentally. Radiation is fed into an air-filled cubical copper cavity 8 ft. on an edge. Strings of thermocouples with alternate junctions coated with a "lossy" material are placed at random in the cavity. The e.m.f. of these thermocouples is proportional to the Q of the cavity and its contents. With the total pressure inside the cavity at one atmosphere, the partial pressure of the water vapor is varied from 1 mm to 55 mm of Hg. A measurement of the change in e.m.f. with humidity yields a value for the losses in the water vapor, provided the Q of the cavity is known. This quantity may be determined from additional measurements taken with an aperture opened in the side of the

cavity. The wave-length range between 0.7 cm and 1.7 cm has been explored. Results indicate a peak at $\tilde{\nu}=0.744 \pm 0.005 \text{ cm}^{-1}$, corresponding to a wave-length $\lambda=1.34 \text{ cm}$. The absorption line is broadened as the water vapor density is increased. At very low density, the half-width of the curve (half-width at half-height) is $0.087 \pm 0.01 \text{ cm}^{-1}$, while the corresponding value for a density of 50 gram/meter³ is $0.107 \pm 0.01 \text{ cm}^{-1}$. The cross section for a water-water collision must be nearly 5 times that for a water-air collision to account for this change in half-width with vapor density. The attenuation at the peak is 0.025 db per kilometer for 1 gram of water vapor per cubic meter.

INTRODUCTION

MEASUREMENTS on the infra-red spectrum of water vapor made by Randall¹ and co-workers and slightly revised by Dennison² indicated an absorption line at $\tilde{\nu}=0.78 \text{ cm}^{-1}$. This line results from a transition between the following rotational energy levels.

J_τ	W/hc
5 ₋₁	446.39 cm^{-1}
6 ₋₅	447.17 cm^{-1}

J determines the total angular momentum of the system. τ is an index which runs from $+J$ to $-J$ and denotes the ordering of the levels as regards their magnitude within any J group. The accuracy here is rather poor, of course, and the infra-red measurements determined $\tilde{\nu}_0$ only within the limits 1.0 cm^{-1} and 0.66 cm^{-1} .

This absorption line is relatively weak. For example, the largest absorption measured in this

experiment is of the order of 1000 times smaller than that measured by Cleeton and Williams³ in their work with ammonia.

The experimental procedure described below is in some respects the electromagnetic analog of the method used by Knudsen⁴ for sound absorption measurements.

THEORY

In this experiment, the absorption by water vapor is determined by a comparison of the energy loss due to water vapor in a large cavity with that due to an aperture in the wall of the cavity. This latter quantity can be calculated from a theoretical formula. The time and space average of the energy density in the cavity is directly dependent on the losses, so that losses due to various absorbers may be compared if a detector is used whose output is proportional to $\langle E^2 \rangle_{Av}$. The detector used in this experiment is a series of thermocouple junctions distributed throughout the cavity, with alternate junctions coated with a lossy material.

The fundamental assumption is that the steady-state response of the thermocouples (hereafter called ϵ) is proportional to the Q of the

† This paper is based on work done for the OSRD under Contract OEMsr-485.

* National Research Council Predoctoral Fellow. Submitted by Gordon E. Becker in partial fulfillment of the requirements for the degree of Doctor of Philosophy in the Faculty of Pure Science, Columbia University. Publication assisted by the Ernest Kempton Adams Fund for Physical Research of Columbia University.

¹ H. M. Randall, D. M. Dennison, Nathan Ginsburg, and Louis R. Weber, *Phys. Rev.* **52**, 160 (1937).

² D. M. Dennison, *Rev. Mod. Phys.* **12**, 189 (1940).

³ C. E. Cleeton and N. H. Williams, *Phys. Rev.* **45**, 234 (1934).

⁴ V. O. Knudsen, *J. Acous. Soc. Am.* **5**, 112 (1933).

box and its contents:

$$\varepsilon \propto Q_{\text{total}}. \quad (1)$$

An examination of the conditions under which this assertion is justified is made by Lamb in the paper immediately following this one. A very important condition is that a large number of normal modes of the box must be excited. Another is that the modes must have essentially the same degree of excitation and absorption. The ultimate check on the validity of (1) is given by the experimental tests mentioned below.

Q is defined by the usual relation

$$Q = \frac{\omega \cdot (\text{energy stored})}{\text{energy lost per second}},$$

where $\omega = 2\pi \cdot (\text{frequency})$. It is convenient to use separate Q -values corresponding to the following losses:

- (1) Q_B : Losses in copper walls, glass tubing and thermocouples, oxygen, etc.
- (2) Q_V : Losses in water vapor.
- (3) Q_A : Losses through an aperture in the wall of the box.

The total Q is then given by

$$\frac{1}{Q_t} = \frac{1}{Q_B} + \frac{1}{Q_V} + \frac{1}{Q_A}.$$

An expression for Q_V may be found by a comparison of the following expressions for the energy decay in the vapor between pulses:

$$W = W_0 \exp(-\omega t / Q_V),$$

$$W = W_0 \exp(-\mu x) = W_0 \exp(-\mu ct);$$

c is the velocity of light, t is the time, μ is the absorption coefficient in units of reciprocal length, and x is the length of path in the absorbing vapor. Thus,

$$1/Q_V = \lambda \mu / 2\pi = K \gamma \lambda, \quad (2)$$

where γ may be expressed in units like db per kilometer, and K depends on the units chosen for γ .

Lamb has shown that the Q of the aperture is given by

$$Q_A = 8\pi V / \lambda A, \quad (3)$$

where V is the volume of the box, and A is the area of the hole. This expression holds as long

as A is not small enough to produce diffraction effects, and not large compared to the wall area.

Thus, by combination of (1), (2), and (3),

$$1/\varepsilon = \eta [(1/Q_B) + K \gamma \lambda + \lambda A / 8\pi V]. \quad (4)$$

The proportionality constant η depends, among other things, on the sensitivity of the thermocouples and on the power output of the source.

EXPERIMENTAL APPARATUS

Figure 1 is a schematic diagram for the microwave spectroscopy. A number of magnetrons of fixed wave-lengths were used in pulsed operation as sources of radiation. Under the operating conditions used, the average power output of these tubes ranged from 5 to 20 watts, and the peak powers from 10 to 40 kilowatts. The radiation is fed into an approximately cubical copper box through a wave guide terminating in a matched horn. The total pressure inside the box

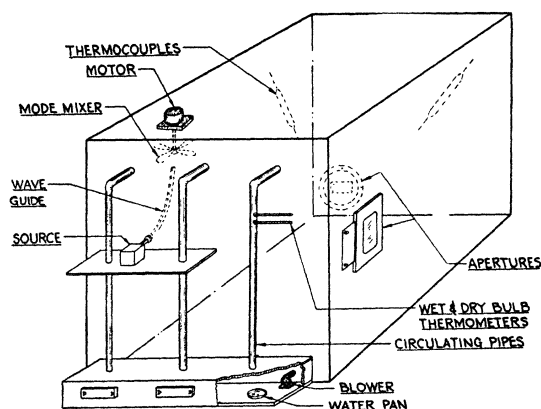


FIG. 1. Diagram of apparatus. Only two thermocouple strings are shown. Actually, the thermocouples are distributed throughout the volume of the box. The copper box is approximately 8 ft. on an edge, with a volume of 15.8 m³. The walls are 0.020 inch thick, approximately plane, and are supported by an outer wooden framework.

is always atmospheric. It is not possible to maintain any appreciable pressure differential between the interior of the box and the room, but the box is sufficiently air-tight so that the water vapor density inside remains reasonably constant at any desired value.

The thermocouple system was changed several times in an effort to obtain a greater e.m.f. and a smaller time constant. In the final version, the Chromel-constantan thermocouples were

made in strings, with the distance between junctions varying between 10 and 15 mm. Flattened wire of 0.025-mm thickness and 0.5-mm width was used. The strings were inclosed in low-loss glass tubes 5 mm in diameter. The pressure

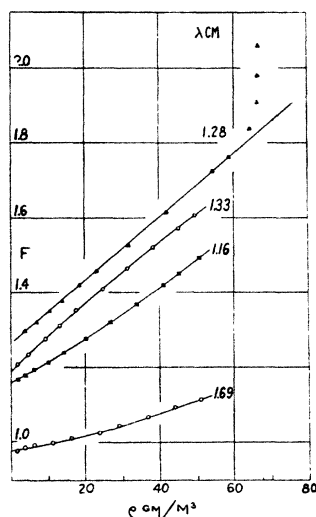


FIG. 2. F vs. ρ curves for several wave-lengths. For values of ρ between 0 and 50 g/m^3 , the curve for $\lambda=1.28$ is a straight line, while the others exhibit upward and downward curvature. The marked departure from linearity of the 1.28 curve above $\rho=60$ g/m^3 is caused by the condensation of water on the walls of the cavity. (The zero-intercepts of these curves should not be compared with each other, because the Q of the box and contents was not the same for all the runs shown.)

inside these tubes is atmospheric, and they are sealed shut, so that the water vapor concentration inside the tube does not change. The total number of pairs of junctions is 360. Alternate junctions are coated with a small amount of a lossy mixture of iron powder in a polystyrene base.

The wave-guide input points at a four-bladed copper fan 2 ft. in diameter, which rotates at a speed of 2 or 3 r.p.s. near the ceiling of the box. This "mode-mixer" is essential for the excitation of all the normal modes and the production of a uniform energy distribution inside the box. There is a similar fan near one of the side walls.

There is a hole cut in each of two side walls of the box. The area of these may be varied from zero to 400 cm^2 . One of them is covered by a thin sheet of celluloid and may be effectively removed by sliding a copper plate in front of the celluloid. This provides an aperture through

which radiation, but not water vapor, may escape. The effective area of the celluloid window is found at each wave-length by comparing the loss through it with the loss through the other aperture (uncovered) at low humidity.

The circulation system is necessary for the maintenance of uniform vapor density and temperature throughout the box.⁵ The air speed in the vertical metal pipes is great enough⁶ so that the humidity may be measured by the use of wet and dry bulb thermometers inserted in one of the pipes. Water vapor may be added to the box by placing shallow pans of water containing electric heaters in the wooden box shown in Fig. 1. The vapor density may be changed from 5 g/m^3 to 50 g/m^3 in 45 minutes by this method,⁷ although smaller steps than this are taken in practice.

The room containing the box is kept at a uniform temperature of $45^\circ\text{C} \pm 1^\circ\text{C}$, so that high absolute humidities may be obtained without danger of condensation of the water vapor. This is accomplished by the use of eight electric fans and heaters distributed about the room. The potentiometers required for measurements are located in an adjoining room.

EXPERIMENTAL PROCEDURE

For the purpose of monitoring the power from the source, a thermocouple junction is mounted

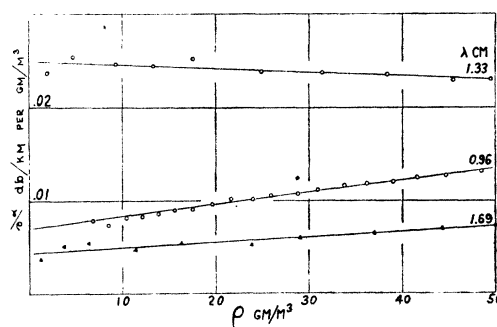


FIG. 3. Attenuation per unit density vs. water vapor density, for several wave-lengths.

⁵ In the cavity itself, the breeze created is sufficiently strong to swing the thermocouple tubes through small distances. This is in no way objectionable, since it helps in the averaging and mode-mixing.

⁶ *Smithsonian Meteorological Tables*, fifth revised edition (1931), page lxx and Table 84.

⁷ Approximately, 1 g/m^3 corresponds to 1 mm of Hg pressure. The dew points corresponding to the densities above are about 1°C and 40°C , respectively.

near the center of a wave guide coming off a tee-section in the main input line. This monitor is subject to long period drifts with room temperature, and is often not reliable if there are large power fluctuations. When the monitor operates satisfactorily, the power from the source can be held constant to within at least 0.2 percent for a period of 20 or 30 minutes by making adjustments in the operating voltage. The following procedure makes the readings independent of the long period power variations, since it eliminates the constant η from the calculations.

The thermocouple e.m.f. ϵ is designated by ϵ_0 for the aperture closed, and by ϵ_A for the aperture open. With the power input and humidity constant, a reading ϵ_0 is taken, and the aperture is then opened. After two minutes, which is sufficient time for the thermocouples to reach equilibrium, a reading ϵ_A is taken, and the aperture is then closed. This procedure is repeated four or five times. With successive values of ϵ_0 and ϵ_A , the quantity

$$F \equiv \epsilon_A / (\epsilon_0 - \epsilon_A) = (8\pi V / \lambda A) \cdot [(1/Q_B) + K\gamma\lambda] = Q_A / Q_{(B+V)} \quad (5)$$

is calculated. The average value of F is used for one point on an F vs. ρ plot. (ρ is the water vapor density in g/m^3 .)

The humidity is then changed, and the procedure repeated. Figure 2 shows examples of F vs. ρ curves. It may be seen from the figure that the curve for $\lambda = 1.28$ cm is straight, that for $\lambda = 1.33$ cm is curved downwards, while the others shown are curved upwards. (Note that if γ is a linear function of ρ , then the F vs. ρ plot is a straight line.)

TABLE I. Attenuation per unit density for various wave-lengths and humidities. Values of γ/ρ are in db/km per g/m^3 , $\tilde{\nu}$ in cm^{-1} , and ρ in g/m^3 .

ρ	$\tilde{\nu} \rightarrow 1.34$	1.16	1.04	0.943	0.859	0.817	0.784	0.751	0.730	0.671	0.592
0	0.0086	0.0067	0.0068	0.0103	0.0142	0.0184	0.0230	0.0249	0.0224	0.0128	0.0044
10	0.0103	0.0081	0.0081	0.0112	0.0149	0.0189	0.0230	0.0245	0.0224	0.0131	0.0049
20	0.0119	0.0095	0.0094	0.0120	0.0157	0.0194	0.0230	0.0241	0.0224	0.0133	0.0055
30	0.0136	0.0108	0.0107	0.0128	0.0165	0.0198	0.0230	0.0237	0.0224	0.0137	0.0060
40	0.0152	0.0122	0.0120	0.0137	0.0172	0.0203	0.0230	0.0234	0.0224	0.0139	0.0066
50	0.0168	0.0136	0.0133	0.0145	0.0179	0.0208	0.0230	0.0230	0.0224	0.0142	0.0071

⁸ The values in Table I will be expressed in the units nepers/cm per g/m^3 if multiplied by the factor 0.2303×10^{-6} . An effective absorption cross section of the water vapor molecule for photons may be defined by the relation $\sigma = 1/n\Lambda$, where n is the number of vapor molecules per unit volume, and Λ is the mean free path for photons in the water vapor. Comparison of the damping terms $\exp(-x/\Lambda)$ and $\exp(-\mu x) = \exp(-k\gamma x)$ gives $\gamma = \text{constant} \cdot (1/\Lambda)$, so that $\sigma = \text{constant} \cdot (\gamma/\rho)$. To find σ in $\text{cm}^2/\text{molecule}$, multiply the values in Table I by the factor 20.6×10^{-24} . Note that this is an effective cross section for all the molecules, not just for the excess in the state 5_{-1} over those in state 6_{-5} .

The intercept F_0 is found by extrapolating these curves to zero humidity ($\gamma = 0$ for $\rho = 0$). The value of γ may be found as follows: from (5), $F_\rho - F_0 = 8\pi VK\gamma/A$. Therefore,

$$\gamma = [A/8\pi VK] \cdot (F_\rho - F_0) \quad (6)$$

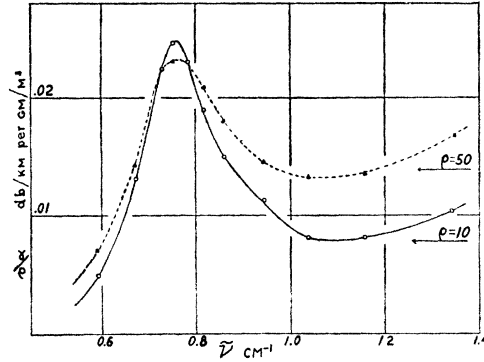


FIG. 4. Water vapor absorption curve. The attenuation in db/kilometer per gram/meter³ is plotted against the wave-number. The dotted curve is for a density of 50 g/m³, the full curve for 10 g/m³.

The quantity γ/ρ (attenuation per unit density) is calculated and plotted against ρ . Figure 3 gives examples of these curves. The points seem to be fitted best by straight lines. Low humidity points are largely disregarded in drawing these straight lines, because they change very rapidly with change in F_0 . Note that, in general, γ/ρ is not a constant, as might have been expected.

The final values of γ/ρ are read off from these straight lines. The values of all runs at each wave-length are averaged, and the absorption curve (γ/ρ vs. $\tilde{\nu}$) is plotted. Figure 4 shows this curve. Table I gives the values found for the attenuation per unit vapor density.⁸

Note that the shape and height of this curve change as humidity changes, even though the total pressure remains constant at one atmosphere.

EXPERIMENTAL CHECKS ON BASIC THEORY

The change in shape of the absorption curve was striking and, also, unexpected. Therefore, attempts were made to check experimentally all

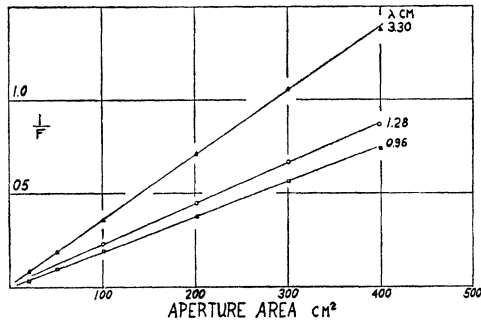


FIG. 5. The fraction $1/F$ vs. the aperture area. Straight lines are drawn through the points.

assumptions and formulas as far as this was possible.

The Aperture

From formula (5)

$$F = (8\pi V/\lambda A) \cdot [(1/Q_B) + (1/Q_V)].$$

For the range of areas for which the formula $Q_A = 8\pi V/\lambda A$ is valid, and for Q_B and Q_V constant, $1/F$ should be proportional to A . Figure 5 shows that this has been verified. The range for A has been extended up to 800 cm² by using both apertures simultaneously. Also, by the use of calibrated celluloid-covered apertures, the relation has been tested at high humidity. No significant departure from linearity has been found.

It is assumed that there is a uniform energy distribution in the box. This was not the case before the copper fans were placed in the box, as was shown by the fact that the Q_A -values were not the same for apertures of equal area in different walls of the box. However, with the fans on, the Q_A -values of the two apertures are the same to within 1 percent.

Effect of Change of Power on F

The fraction F is supposed to be independent of power output of the source, provided that the power output is constant during the determination of F . This can be checked by measuring F , and then, with humidity constant, changing the power output and measuring F again. This was done at two wave-lengths. The power was changed by more than 30 percent; and the variations in F were smaller than the probable experimental error.

Effect of Pulse Length and Pulse Repetition Rate

The quantity F should be independent of the pulse duration and repetition rate, provided that the thermocouples do not saturate during a pulse, and provided that the effect of the pulse duration on the number of normal modes excited is not important. When the pulse length was changed from $\frac{1}{4}$ μ sec. to $\frac{1}{2}$ μ sec., and the repetition rate from 2000 per sec. to 1000 per sec., the variations in F were smaller than the probable experimental error.

Q_B -Values

By use of values of the intercept F_0 of the F vs. ρ curves, values of Q_B may be obtained.

$$F_0 = (8\pi V/\lambda A) \cdot (1/Q_B).$$

Table II gives values of Q_B found in this way for a set of runs using the same experimental arrangement of materials inside the box. If only copper losses were present, the product $Q_B\lambda^{\frac{1}{2}}$ should be a constant. The small departures shown in the table are reasonable, since the box contains non-metallic substances, e.g., the glass tubes surrounding the thermocouples.

The values of Q_B are about 50 percent below the theoretical value for a copper cavity. Measurements show that the glass tubes, thermocouples, screening, etc. account for about 20 percent, and the remaining discrepancy is about what is usually found for copper cavities or wave guides.

TABLE II. Values of $Q_B\lambda^{\frac{1}{2}}$.

λ (cm)	0.96	1.06	1.16	1.28	1.37	1.49	1.69
$Q_B\lambda^{\frac{1}{2}} \times 10^{-3}$	8.05	8.04	8.14	7.95	7.98	7.93	7.84

Variations of Wall Losses with Humidity

The γ vs. ρ curves have a form which approximates $\gamma = a\rho + b\rho^2$. It was thought possible that the coefficients of the linear and squared terms might be partly determined by losses in some kind of water layer absorbed on the walls of the box. If this were true, these losses should be proportional to the area of copper exposed to the radiation, and the addition of copper surface should increase any curvature present in the γ vs. ρ plot.

This experiment was conducted at $\lambda = 0.96$ cm by placing a number of sheets of copper inside the box. Figure 6 shows the results. The full line is a least-square parabola for several normal runs. Note that points for copper added fall slightly below the curve, with some falling on it. The results are not as clear-cut as might be desired, but there is no evidence that the points for the box with added copper sheets fall higher than those for the normal box. To indicate the magnitude of the change which might be expected when the copper sheets are added, the dashed curve in the figure has been calculated on the assumption that the coefficient of ρ^2 arises entirely from losses in a water layer on the copper. (Note that there is also no evidence of a change in the coefficient of the linear term.)

Figure 2 illustrates what happens when the humidity is raised until water condenses on the walls. This condensation does not take place at

TABLE III. Percent average deviation of the values averaged for γ/ρ .

$\bar{\nu}$	1.34	1.16	1.04	0.943	0.859	0.817	0.784	0.751	0.730	0.671	0.592	
ρ	10	3.9	3.8	6.4	6.2	2.8	1.4	0.7	1.6	1.4	2.9	9.4
	50	±1.7	1.6	2.4	2.1	0.5	0.4	0.7	0.5	1.4	1.9	2.6

the same instant for all parts of the walls, because there is usually as much as $\frac{1}{2}^\circ\text{C}$ variation of wall temperature from one point to another. This is the probable explanation for the part of the curve between 55 and 60 g/m³.

PRECISION OF MEASUREMENTS

Measurements of humidity made by the use of wet and dry bulb thermometers are probably correct to within ± 0.3 g/m³. Checks were made

by the use of a dew point apparatus, and the values found agreed to within ± 0.5 g/m³. The dew point, as observed with this apparatus, was not sharply defined, however, and this uncer-

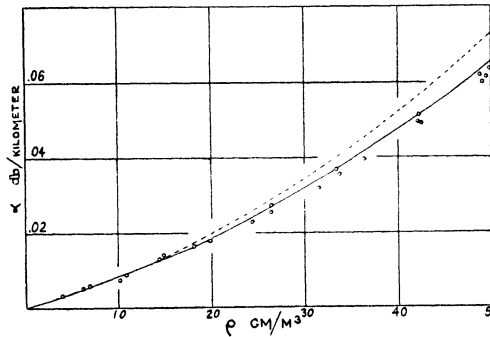


FIG. 6. Attenuation vs. vapor density for a wave-length of 0.96 cm. The points shown are for cases with added copper surface in the cavity. The full line is a parabola fitted to the average of points from several normal runs. The equation for it is $\gamma = 0.0127\rho + 2.26 \times 10^{-4}\rho^2$. The dotted line is given by the equation $\gamma = 0.0127\rho + (504/408) \times 2.26 \times 10^{-4}\rho^2$. That is, the coefficient of the squared term has been increased by a factor which is the ratio of the copper surfaces with and without the added copper.

tainty was great enough to explain the differences observed.

The value of Q_A is probably correct to within ± 1 percent.

The values for (γ/ρ) shown on the absorption curve were found by averaging results from data taken over a period of several months, during which time several different thermocouple systems were used. Results from data taken after improvements were made in the thermocouple system were given more weight in the averaging. Table III gives the percent average deviation of the values of (γ/ρ) which were averaged to find the values for Table I.

It is seen that the self-consistency of the results is better for higher value of attenuation, and that, in general, it is better for values at $\rho = 50$ than at $\rho = 10$. We estimate that the probable error is within ± 5 percent for the high values of attenuation, and nowhere exceeds ± 10 percent.

DISCUSSION OF RESULTS

Van Vleck⁹ gives the following formula for

⁹ J. H. Van Vleck, NDRC Reports 664 and 43-2. See also J. H. Van Vleck and V. F. Weisskopf, Rev. Mod. Phys. 17, 227 (1945).

water vapor absorption in this wave-length range,

$$\frac{\gamma}{\rho} = C_1 \bar{\nu}^2 \left\{ \frac{\Delta\nu/c}{(\bar{\nu} - \bar{\nu}_0)^2 + (\Delta\nu/c)^2} + \frac{\Delta\nu/c}{(\bar{\nu} + \bar{\nu}_0)^2 + (\Delta\nu/c)^2} \right\} + C_2 \bar{\nu}^2 (\Delta\nu/c); \quad (7)$$

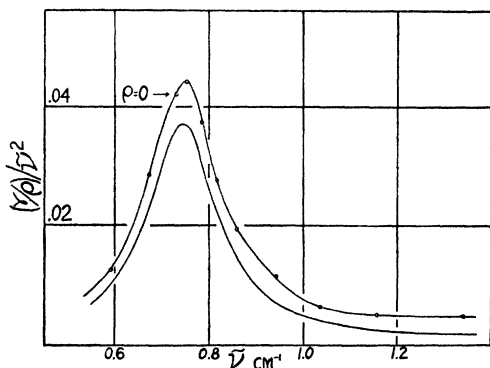


FIG. 7. These curves are obtained from the absorption curve (Fig. 4) by dividing each ordinate by the square of the corresponding wave number. The upper curve is the experimental curve for very low density. The resonant wave number and the half-width found from this curve are 0.744 cm^{-1} and 0.087 cm^{-1} , respectively. The lower curve is the theoretical curve obtained from Eq. (7) when the experimental values of $\bar{\nu}_0$ and $(\Delta\nu/c)$ are used.

$(\Delta\nu/c)$ is the half-width at half-height of the absorption line. $\bar{\nu}$ is the wave number of the incident radiation. $\bar{\nu}_0$ is the resonant wave number. The values of C_1 and C_2 depend on the units used for γ .

It is seen from (7) that the resonance curve is not symmetrical, mainly because γ is proportional to $\bar{\nu}^2$. For the purpose of determining $\bar{\nu}_0$ and $\Delta\nu/c$, it is convenient to plot $(\gamma/\rho)/\bar{\nu}^2$ vs. $\bar{\nu}$. Figures 7 and 8 show these curves for experimental points at low and high density, respectively. (Points for $\rho=0$ are found by extrapolation. See Fig. 3.) Values of $\bar{\nu}_0$ and $(\Delta\nu/c)$ were found from these curves, and these values were then used in Eq. (7). These theoretical curves are shown in Figs. 7 and 8. The curves are approximately flat at frequencies off resonance. Here the absorption is largely caused by absorption lines at frequencies greater than 5 cm^{-1} , whose effect is given by the second term in (7).

Figures 9 and 10 show the results of matching the curves in Figs. 7 and 8, respectively, at

$\bar{\nu} = 1.34 \text{ cm}^{-1}$ by subtracting from each curve the value of its ordinate at this value of $\bar{\nu}$. The discrepancies here are not much larger than the probable experimental error, which means that the first term in (7) is in good agreement with experiment. The theoretical curve would fit the experimental points better if this term were multiplied by a factor of about 1.10 for the case of low density, and 1.13 for high density. The chief discrepancy between theory and experiment

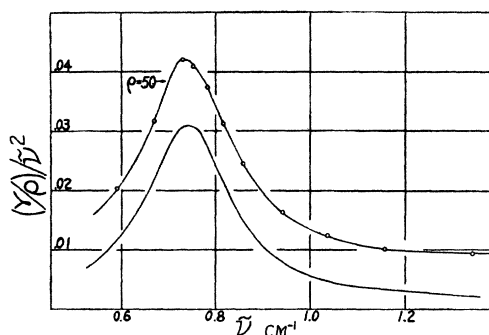


FIG. 8. Same as Fig. 7, for the case of high vapor density. The values of $\bar{\nu}_0$ and $(\Delta\nu/c)$ are 0.742 cm^{-1} and 0.107 cm^{-1} , respectively.

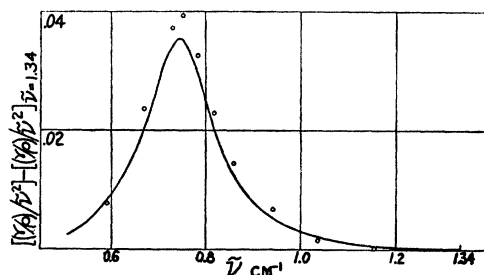


FIG. 9. This curve results from matching the curves of Fig. 7 at $\bar{\nu} = 1.34 \text{ cm}^{-1}$ by subtracting from each curve the value of its ordinate at this value of $\bar{\nu}$. This arbitrary value of $\bar{\nu}$ is selected because the curves are nearly flat here. The full line is the theoretical curve, and the points shown represent experimental data.

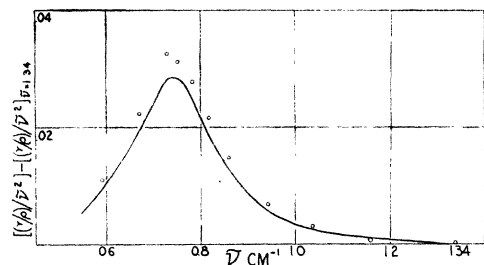


FIG. 10. This curve results from matching the curves of Fig. 8 (high density), as explained under Fig. 9.

is in the magnitude of the nearly constant absorption in this region due to strong lines at higher frequencies. The second term in Eq. (7) must be multiplied by factors of about 4 and 6 (for the cases of low and high density, respectively) to produce agreement with experiment. These factors are not determined with great accuracy, however.

Figure 11 shows clearly that the absorption line is broadened as the water vapor density is increased. The values of $\Delta\nu/c$ for low and high density are 0.087 cm^{-1} and 0.107 cm^{-1} , respectively. These are in good agreement with the value $0.11 \text{ cm}^{-1} \pm 0.02 \text{ cm}^{-1}$ reported by Adel¹⁰ for the half-width of the water vapor line at 15.99μ .

The increase in half-width with increase in vapor density indicates that the cross section for collisions of water molecules with water molecules is greater than that for collisions of water molecules with air molecules. Let σ_{WW} and σ_{WA} denote the two cross sections. The effective cross section at a given value of ρ is then $\sigma_{WW} \cdot q_\rho + \sigma_{WA} \cdot (1 - q_\rho)$, where q_ρ is the fraction of molecules which are water. The effective cross section increases by a factor 1.23 as ρ increases from 0 to 50 g/m^3 . With these values, $\sigma_{WW} = 4.7\sigma_{WA}$.

¹⁰ A. Adel, NDRC Report 320, and later unpublished results.

Measurements by other methods have been reported by Dicke and co-workers¹¹ and by Miller and Bender.¹² Their results agree with those given here within the limits of experimental error. However, these other methods are not capable of detecting a change in shape of the absorption line with vapor pressure.

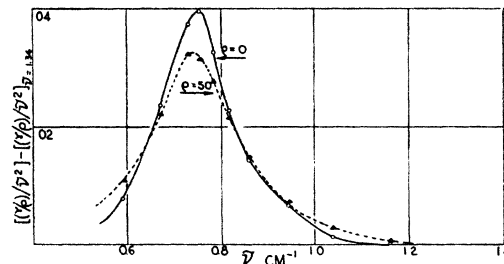


FIG. 11. Experimental curves are shown, of the same type as in Figs. 9 and 10. They correspond to the limiting values of the water vapor density used in this experiment.

Many thanks are due Professor J. M. B. Kellogg for his invaluable assistance and guidance throughout the course of this experiment. We are also indebted to Professor W. E. Lamb for much helpful discussion.

¹¹ R. H. Dicke, R. L. Kyhl, A. B. Vane, and E. R. Beringer, NDRC Report 1002. See also, *Bull. Am. Phys. Soc.* **21**, 25 (1946).

¹² J. W. Miller and R. S. Bender, NDRC Report 729.